Available online at www.sciencedirect.com
SCIENCE DIRECT®
PERGAMON
International Journal of Heat and Mass Transfer 46 (2003) 4051–4057
International Journal of HEAT and MASS TRANSFER
www.elsevier.com/locate/ijhmt

A void fraction model for annular flow in horizontal tubes

Todd M. Harms *, Daqing Li, Eckhard A. Groll, James E. Braun

Purdue University, 1077 Ray W. Herrick Laboratories, West Lafayette, IN 47907, USA

Received 4 October 2002; received in revised form 11 April 2003

Abstract

An important feature of detailed system simulation models for unitary air conditioners is the calculation of charge inventory. Void fraction determination in the two-phase regions of the heat exchangers is the primary challenge associated with charge inventory calculations. Annular flow is one of the predominant flow regimes encountered in horizontal heat exchangers. Analytical annular flow models typically fail to accurately represent void fraction. Thus, many of the available void fraction models are empirically based. To improve the prediction capabilities of void fraction models, a mechanistic void fraction model has been developed for annular flow in horizontal tubes. The present model considers the effect of momentum eddy diffusivity damping at the liquid–vapor interface. Two approaches are presented for determining the wall shear stress. The modeling results are compared to predictions from various void fraction models found in the literature. The present model is found to work well at moderate mass fluxes.

1. Introduction

The slip flow model is commonly used to analyze two-phase flow. The slip flow model assumes that at each cross-section: the phases are separated into two distinct regions, the velocity across each phase is uniform, and the pressure is uniform. One of the major challenges in utilizing the slip flow model is the determination of the void fraction. A separate analysis is needed to provide void fraction predictions. Separate regime specific models, such as an annular flow model, can be used to generate the required predictions.

A specific application of void fraction modeling is in system simulation models for air conditioners. Detailed simulation models of air conditioners require the determination of the system charge inventory. Charge inventory is the accounting of distributed mass in a two-phase system. If the void fraction is known in the two-phase sections of the heat exchangers, then the charge inventory can be calculated in a straightforward manner.

A summary of the approaches typically taken to model void fraction in the air conditioning industry is given in Table 1. The earlier models were identified in a review of the literature [9]. Many of the studies consider the flow to be separated, while some of the studies are regime specific. The models are analytical, semi-empirical, or empirical. Given the complexity of two-phase flow, only very simple models are completely analytical. Here, models are deemed semi-empirical if they are essentially analytical, but utilize empirical closure equations or fitted constants. Two-phase empirical models often assume a functional form or a set of dimensionless parameters, and have constants that are determined from experimental data. As expected of models that are popular for design work, most of the correlations are explicit functions of measurable quantities.

Many of the commonly used correlations are empirically based. Furthermore, generalized solution methods are iterative or are otherwise too complicated to be used as design tools. The present study takes the approach of a regime specific model for annular flow. The present study will improve upon the current state of the art in that it will be explicit, analytical expression. The major drawback of this approach is that the new correlation will only apply over a limited range of operating parameters.

* Corresponding author.

0017-9310/03/$ - see front matter © 2003 Published by Elsevier Ltd.
doi:10.1016/S0017-9310(03)00228-X

Nomenclature

A	cross-sectional area, m^2
A^+	empirical constant
D	diameter, m
e^+	dimensionless eddy diffusivity
f	friction factor
Fr_{TD}	modified Froude number
g	gravitational acceleration, m/s^2
G	mass flux, $kg/(m^2\,s)$
p	pressure, Pa
r	radial coordinate, m
R	tube radius, m
Re	Reynolds number
S	slip ratio
u	axial velocity, m/s
u_*	friction velocity, m/s
x	quality
X_{tt}	Lockhart–Martinelli parameter
y	wall coordinate, m
z	axial coordinate, m

Greek symbols

α	void fraction
δ	film thickness, m
ε_m	momentum eddy diffusivity, m^2/s
ϕ	pressure drop multiplier
κ	empirical constant
μ	dynamic viscosity, $kg/(m\,s)$
ν	kinematic viscosity, m^2/s
ρ	density, kg/m^3
τ	shear stress, Pa

Superscript

+	dimensionless qualifier

Subscripts

f	liquid
g	vapor
i	interfacial
w	wall

2. Analytical model

A schematic of two-phase annular flow in a circular tube is given in Fig. 1. The axial coordinate, z, is indicated in the figure, as well as two sets of coordinate variables perpendicular to the flow. The wall coordinate, y, is complimentary to the radial coordinate, r, as given by Eq. (1)

$$y = R - r \tag{1}$$

where R is the tube radius. The flow is assumed to be one-dimensional and adiabatic. Some of the complexities associated with annular flow (interfacial waves and entrainment) have been neglected.

Void fraction, α, is defined as the fraction of area occupied by vapor at a given cross-sectional location, Eq. (2)

$$\alpha = \frac{A_g}{A} \tag{2}$$

where A is the cross-sectional area of the tube and A_g is the area occupied by vapor at that cross-section. This expression can be rewritten in terms of the given coordinate system, Eq. (3).

$$\alpha = \left(1 - \frac{\delta}{R}\right)^2 \tag{3}$$

where δ is the film thickness. The primary challenge is determining the film thickness.

The analysis proceeds with a control volume approach of annular flow in a circular tube. The orientation of the tube is taken to be horizontal as the evaporators and condensers found in air conditioners are almost exclusively arranged in this manner. As in-

Table 1
Summary of void fraction models

	Regime	Correlation	Form	Notes
Homogeneous		Analytical	Explicit	$S = 1$
Zivi [16]	Separated	Analytical	Explicit	No friction
Smith [10]	Separated	Semi-empirical	Explicit	No friction
Baroczy [2]	Separated	Empirical	Tabular	Vertical upflow
Premoli et al. [8]	Separated	Empirical	Explicit	Vertical upflow
Yashar et al. [15]	Separated	Empirical	Explicit	Horizontal
Hughmark [5]	Bubble	Empirical	Implicit	Vertical upflow
Taitel and Barnea [12]	Slug	Semi-empirical	Explicit	
Tandon et al. [13]	Annular	Semi-empirical	Explicit	

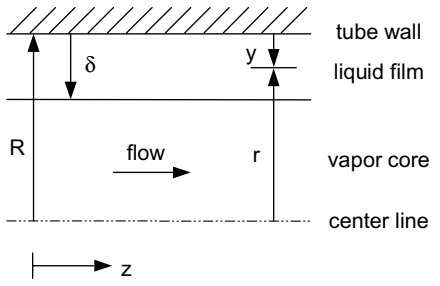

Fig. 1. Schematic of two-phase annular flow in a circular tube.

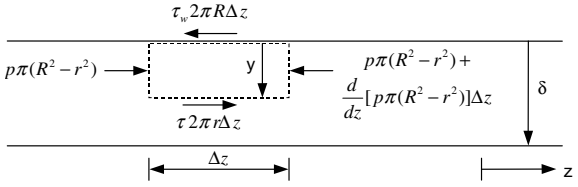

Fig. 2. Control volume analysis of annular flow in a horizontal tube.

dicated in Fig. 2, a control volume analysis of the liquid film yields the following,

$$\tau = \tau_w \frac{R}{r} - \frac{1}{2}\frac{dp}{dz}\frac{R^2 - r^2}{r} \tag{4}$$

where τ is the shear stress in the liquid film at location r, τ_w is the wall shear stress, and p is the pressure. Similarly, a control volume analysis of the entire flow yields the following,

$$\tau_w = -\frac{R}{2}\frac{dp}{dz} \tag{5}$$

Combining Eqs. (4) and (5) gives a relationship, Eq. (6), between the shear stress in the liquid film and the wall shear stress.

$$\tau = \left(1 - \frac{y^+}{R^+}\right)\tau_w \tag{6}$$

where the dimensionless terms, y^+ and R^+, are defined by Eqs. (7) and (8), respectively. Notice that for a relatively thin liquid film, the shear stress in the liquid film is nearly equal to the wall shear stress. This result is in sharp contrast to gravity-driven film flow, where the interfacial shear stress is nearly zero.

$$y^+ = \frac{yu_*}{\nu_f} \tag{7}$$

$$R^+ = \frac{Ru_*}{\nu_f} \tag{8}$$

where the friction velocity is defined as follows,

$$u_* = \left(\frac{\tau_w}{\rho_f}\right)^{1/2} \tag{9}$$

For turbulent flow, shear stress is defined as

$$\tau = \mu_f\left(1 + \frac{\varepsilon_m}{\nu_f}\right)\frac{du}{dy} \tag{10}$$

where ε_m is the momentum eddy diffusivity and u is the axial velocity. Eq. (10) can be combined with Eq. (6) to yield,

$$\frac{du^+}{dy^+} = \frac{1}{1+e^+}\left(1 - \frac{y^+}{R^+}\right) \tag{11}$$

where u^+ and e^+ are defined in Eqs. (12) and (13), respectively.

$$u^+ = \frac{u}{u_*} \tag{12}$$

$$e^+ = \frac{\varepsilon_m}{\nu_f} \tag{13}$$

As shown in Eq. (14), a model for e^+ has been developed for shear-driven liquid films following the procedure described by Mudawar and El-Masri [7] concerning the development of a momentum eddy diffusivity model for gravity-driven liquid films.

$$\frac{\varepsilon_m}{\nu_f} = -\frac{1}{2} + \frac{1}{2}\left\{1 + 4\left[1 - \exp\left(\frac{-y^+}{A^+}\right)\right]^2\left[\kappa y^+\left(1 - \frac{y^+}{\delta^+}\right) + \kappa^2 y^{+2}\left(1 - \frac{y^+}{\delta^+}\right)^2\right]\right\}^{1/2} \tag{14}$$

This can be compared to the case for single-phase turbulent flow proposed by van Driest [3],

$$\frac{\varepsilon_m}{\nu_f} = -\frac{1}{2} + \frac{1}{2}\left\{1 + 4\left[1 - \exp\left(\frac{-y^+}{A^+}\right)\right]^2\kappa^2 y^{+2}\right\}^{1/2} \tag{15}$$

In both cases, $\kappa = 0.4$ and $A^+ = 26$. The dimensionless film thickness, δ^+, is defined as follows,

$$\delta^+ = \frac{\delta u_*}{\nu_f} \tag{16}$$

The van Driest model for momentum eddy diffusivity is compared to the present formulation in Fig. 3. The most striking difference is that the eddy diffusivity for the van Driest model rises monotonically, while in the present model the eddy diffusivity is completely damped out at the interfacial boundary. Furthermore, for the present model, eddy diffusivity additionally depends on the film thickness.

Numerically integrating Eq. (11) gives the local velocity in the liquid film. Note that the ratio y/R has been taken to be approximately one. This assumption limits the range of application to standard tubes. Microchannel

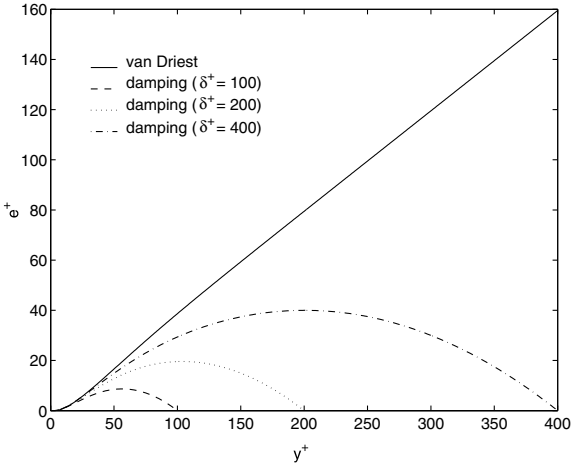

Fig. 3. A comparison of analytical models for dimensionless momentum diffusivity.

and millichannel tubes should not be analyzed with this approach. The film velocity for the two models is compared in Fig. 4. As expected, the interfacial velocity is much higher for the present model. The lack of momentum eddies increases the velocity gradient near the film interface as compared to the single-phase results. As with eddy diffusivity, the liquid velocity for the present model depends on the film thickness.

Mass conservation in the liquid film gives the following,

$$Re_f = 4\int_0^{\delta^+} u^+\left(1-\frac{y^+}{R^+}\right)\mathrm{d}y^+ \tag{17}$$

where the liquid Reynolds number is defined as,

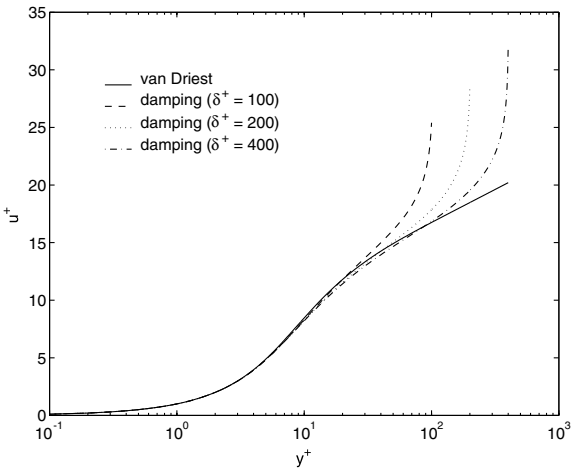

Fig. 4. A comparison of analytical models for dimensionless liquid film velocity.

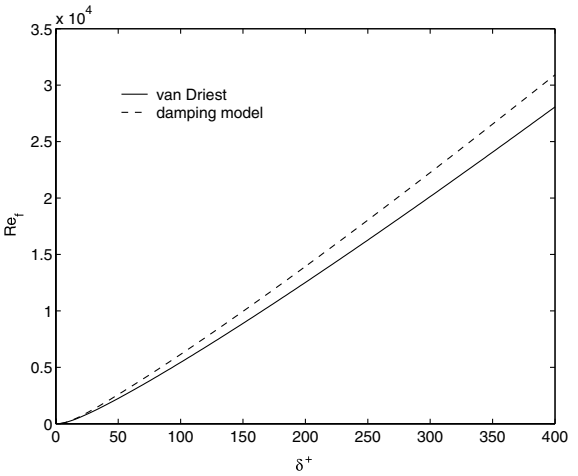

Fig. 5. Liquid Reynolds number as a function of dimensionless liquid film thickness.

$$Re_f = \frac{(1-x)GD}{\mu_f} \tag{18}$$

where x is the mass quality, G is the mass flux, and D is the tube diameter. Numerical integration of Eq. (17) yields the liquid Reynolds number as a function of dimensionless film thickness. The results of that integration are shown in Fig. 5 for the present model and the single-phase case. Again, the ratio y/R has been taken to be approximately one. As a result of the higher velocities in the liquid film, the present model predicts a higher liquid Reynolds number for a given film thickness. The results of the present model can be fit to Eq. (19) with a maximum error of 2%.

$$\delta^+ = \left(1.74 + 0.104 Re_f^{0.5}\right)^2 \tag{19}$$

Using Eq. (19), the remaining challenge is to determine the shear stress. Two general approaches are presented here: an explicit approach and an implicit approach.

2.1. Explicit modeling closure approach

The explicit approach follows the development suggested by Lockhart and Martinelli [6].

$$\tau_w = \frac{f}{2}(1-x)^2\frac{G^2}{\rho_f}\phi_f^2 \tag{20}$$

where according to the Blasius solution, the friction factor for moderate Reynolds numbers is given as [3],

$$f = 0.0791 Re_f^{-0.25} \tag{21}$$

For the two-phase frictional pressure drop multiplier, deSouza et al. [4] recommends,

$$\phi_f = \left(1.376 + \frac{7.242}{X_{tt}^{1.655}}\right)^{1/2} \quad (22)$$

for use in the annular flow regime, where the Lockhart–Martinelli parameter is defined as,

$$X_{tt} = \left(\frac{1-x}{x}\right)^{0.9}\left(\frac{\rho_g}{\rho_f}\right)^{0.5}\left(\frac{\mu_f}{\mu_g}\right)^{0.1} \quad (23)$$

2.2. Implicit modeling closure approach

The second method involves relating the interfacial shear stress, Eq. (24), to the interfacial friction factor.

$$\tau_i = \frac{f_i G^2 x^2}{2\rho_g \alpha^2} \quad (24)$$

where the interfacial friction factor, Eq. (25), can be correlated to Nikuradse's data in the fully rough regime [3]. The sand grain roughness has been taken to be equal to the film thickness. This is in contrast to the recommendation of Wallis [14] of a 4δ equivalent sand grain roughness.

$$f_i = \left[1.74 \ln\left(\frac{D-2\delta}{\delta}\right) + 2.28\right]^{-2} \quad (25)$$

All of the equations in the second routine depend on either the void fraction or the film thickness. Therefore, a numerical solution is required.

3. Results and discussion

A flow regime map should be consulted to ensure that annular flow has been achieved for a given set of operating parameters. While many researchers have reported flow regime maps, most are empirically based. One notable exception is the work by Taitel and Dukler [11]. Their map is developed from a mechanistic approach to flow regime transitions.

The Taitel–Dukler map is shown in Fig. 6. They found that several of the transitions can be described by the Froude number, Eq. (26), and the Lockhart–Martinelli parameter.

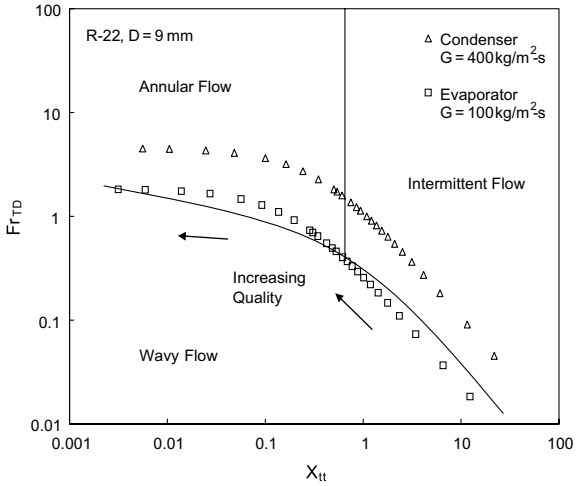

Fig. 6. The Taitel and Dukler flow regime map for two-phase flow in horizontal tubes.

$$Fr_{TD} = \frac{xG}{[\rho_g(\rho_f - \rho_g)gD]^{0.5}} \quad (26)$$

Simulated results are also shown in Fig. 6 for horizontal heat exchangers with R-22 as the working fluid. For the indicated mass flux the pressure was set to 650 and 2000 kPa, to simulate conditions in an evaporator and in a condenser, respectively. The quality ranged from 0.01 to 0.99. By comparison with the simulated results, the wavy flow transition boundary was found to be a strong function of mass flux. Conversely, the intermittent flow to annular flow transition is by definition only a function of the Lockhart–Martinelli parameter, which is in turn a strong function of quality. Barnea et al. [1] suggested an improved transition equation, Eq. (27), based on experimental evidence.

$$X_{tt} = 0.653 \quad (27)$$

This transition provides a lower bound on mass quality for annular flow models. Table 2 lists this lower bound

Table 2
The minimum mass quality allowed by the intermittent-annular flow transition and the liquid Reynolds number range for refrigerants common to the air conditioning industry

	Minimum mass quality		Re_f[a]	
	$T = 5$ °C	$T = 65$ °C	@ x_{min}	@ $x = 0.96$
R-22	0.196	0.389	3600	180
R-410A	0.237	0.485	4350	230
R-134a	0.175	0.365	2850	140
CO_2	0.386	–[b]	5660	380

[a] $T = 5$ °C, $D = 9$ mm, $G = 100$ kg/m² s.
[b] 65 °C is above the critical point for CO_2.

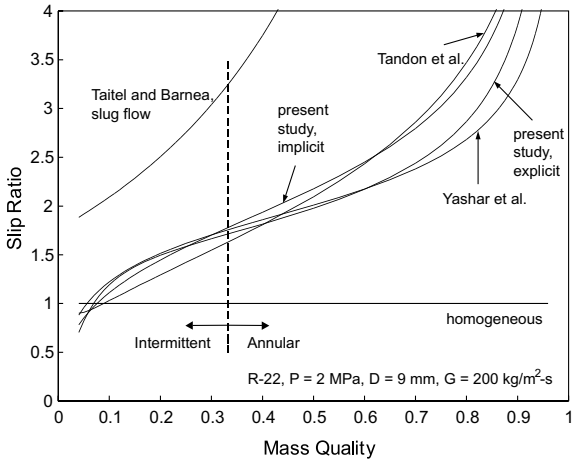

Fig. 7. A comparison of slip ratio predictions for several void fraction models.

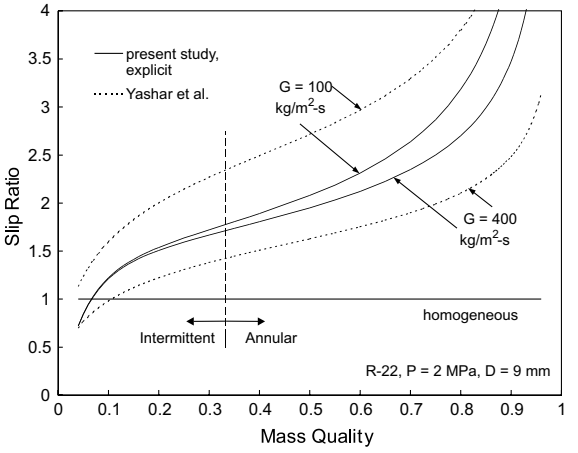

Fig. 8. A comparison of slip ratio predictions examining the effect of mass flux.

for several refrigerants commonly used in the air conditioning industry. For the range of temperatures that occur in air conditioning applications, the lower bound varies from 0.175 to 0.485. The range of liquid Reynolds number is also given Table 2. Notice that the liquid phase is turbulent across most of the range, and only becomes laminar at very high quality.

In Fig. 7, both of the presented methods are compared to selected models from the literature in terms of slip ratio as a function of mass quality. The slip ratio, Eq. (28), provides a physical interpretation of the results.

$$S = \frac{u_g}{u_f} \tag{28}$$

When the void fraction is known or has been calculated, Eq. (29) can be used to determine the slip ratio.

$$S = \frac{\rho_f}{\rho_g}\left(\frac{x}{1-x}\right)\left(\frac{1-\alpha}{\alpha}\right) \tag{29}$$

A void fraction model for slug flow has been included to demonstrate the influence of flow regime. Compared to annular flow models, the slug flow model predicts a much higher slip ratio. The liquid slugs account for the large difference in void fraction predictions between annular flow and slug flow. As expected, the homogeneous model greatly underpredicts the slip ratio across the entire range of mass quality. The three annular flow models compared in Fig. 7 yield similar results. Nonetheless, the explicit method from the present study agrees best with Yashar model. The Tandon model overpredicts slip ratio compared to the present explicit method. This is expected, considering that Tandon used a universal velocity profile for the liquid film. Recalling the results from Fig. 5, damping the eddy diffusivity near the film interface decreases the film thickness, and consequently decreases the slip ratio.

Owing to the improved agreement with the empirical void fraction model and the ease of application of the model, the explicit model is recommended over the implicit model for design purposes. By combining Eqs. (3), (9), (16), and (18)–(22) the explicit model can be represented as follows,

$$\alpha = \left[1 - 10.06 Re_f^{-0.875}\left(1.74 + 0.104 Re_f^{0.5}\right)^2 \times \left(1.376 + \frac{7.242}{X_{tt}^{1.655}}\right)^{-1/2}\right]^2 \tag{30}$$

The explicit method given by Eq. (30) is compared to the empirical model by Yashar et al. [15] in Fig. 8 at mass fluxes of 100 and 400 kg/(m^2 s). While for both models the slip ratio decreases as the mass flux increases, the Yashar model exhibits a much greater dependence on mass flux. The overprediction at high mass flux by the present model can be explained by entrainment processes. As the mass flux increases, the vapor core is more likely to shear off the crests of the liquid waves and entrain them as liquid droplets. As the droplets move at nearly the same velocity as the vapor core, the slip ratio decreases. As the mass flux decreases gravity begins to stratify the liquid, decreasing the gas core shear. The decrease in shear is due to the decrease in gas core surface area compared to annular flow. This leads to the present model underpredicting the slip ratio at low mass fluxes compared to what the experimentally-based Yashar model suggests.

4. Conclusions

A new void fraction model for annular flow in horizontal tubes is presented. Contrary to previous studies, damping of the momentum eddy diffusivity at the film interface is considered. The present results show that interfacial damping of the momentum eddy diffusivity cannot be neglected. Compared to the van Driest model, the film thickness is decreased.

Two closure methods are suggested; one is implicit, while other is explicit. The present explicit model agrees well with an empirical model based on horizontal two-phase flow at moderate mass flux levels. Annular flow models do not show a large dependence on mass flux, while empirical models suggest that a significant dependence exists. Some physical mechanisms are suggested as possible reasons for the disagreement in the models.

References

[1] D. Barnea, O. Shoham, Y. Taitel, Flow pattern transition for downward inclined two phase flow; horizontal to vertical, Chem. Eng. Sci. 37 (1982) 735–740.
[2] C.J. Baroczy, Correlation of liquid fraction in two-phase flow with application to liquid metals, Chem. Eng. Prog. Symp. Ser. 61 (57) (1965) 179–191.
[3] A. Bejan, Convection Heat Transfer, 2nd ed., John Wiley and Sons, New York, 1995.
[4] A.M. deSouza, J.C. Chato, J.P. Wattelet, Pressure drop during two-phase flow of refrigerants in horizontal smooth tubes, ACRC TR-25, University of Illinois, Urbana-Champaign, 1992.
[5] G.A. Hughmark, Holdup in gas–liquid flow, Chem. Eng. Prog. 58 (1962) 62–65.
[6] R.W. Lockhart, R.C. Martinelli, Proposed correlation of data for isothermal two-phase, two-component flow in pipes, Chem. Eng. Prog. 45 (1949) 39–48.
[7] I. Mudawar, M.A. El-Masri, Momentum and heat transfer across freely-falling turbulent liquid films, Int. J. Multiphase Flow 12 (1986) 771–790.
[8] A. Premoli, D. Di Francesco, A. Prina, Una correlazione adimensionale per la determinazione della densità di miscele bifasiche, La Termotecnica 25 (1971) 17–26.
[9] C.K. Rice, The effect of void fraction correlation and heat flux assumption on refrigerant charge inventory predictions, ASHRAE Trans. 93 (1) (1987) 341–367.
[10] S.L. Smith, Void fractions in two-phase flow: a correlation based upon an equal velocity head model, Proc. Inst. Mech. Eng. 184 (1969) 647–664.
[11] Y. Taitel, A.E. Dukler, A model for predicting flow regime transitions in horizontal and near horizontal gas–liquid flow, AIChE J. 22 (1976) 47–55.
[12] Y. Taitel, D. Barnea, Two-phase slug flow, Adv. Heat Transfer 20 (1990) 83–132.
[13] T.N. Tandon, H.K. Varma, C.P. Gupta, A void fraction model for annular two-phase flow, Int. J. Heat Mass Transfer 28 (1985) 191–198.
[14] G.B. Wallis, One-dimensional Two-phase Flow, McGraw-Hill, New York, 1969.
[15] D.A. Yashar, M.J. Wilson, H.R. Kopke, D.M. Graham, J.C. Chato, T.A. Newell, An investigation of refrigerant void fraction in horizontal, microfin tubes, HVAC&R Res. 7 (2001) 67–82.
[16] S.M. Zivi, Estimation of steady-state steam void-fraction by means of the principle of minimum entropy production, J. Heat Transfer 86 (1964) 247–252.